ISPRS Journal of Photogrammetry and Remote Sensing, Volume 60, Issue 6, September 2006, pp. 363-374.

The ADS40 Vaihingen/Enz geometric performance test

Michael Cramer
Institut für Photogrammetrie (ifp), Universität Stuttgart
Geschwister-Scholl-Str. 24d, D-70174 Stuttgart/Germany
michael.cramer@ifp.uni-stuttgart.de

Abstract

This paper presents the main results of the comprehensive ADS40 performance analysis from the test field Vaihingen/Enz, which is one example of an independent in-flight performance study for one of the new and already commercially used digital airborne camera systems. Based on a large number of well coordinated and defined object points, which may serve as independent check points, the absolute geometric accuracy of ADS40 from true operational data is verified. From empirical analysis the ADS40 geometric accuracy potential was proven to be in the range of 1-2µm · m_b (image scale) for horizontal coordinates and 0.03-0.05‰ of flying height for vertical components from 1500m-4000m flying height. This is fully within specification for airborne imaging.

Keywords: ADS40, push-broom, georeferencing, performance, GPS/inertial

1. Introduction

The need for empirical analysis of photogrammetric sensors within specially designed photogrammetric test fields is mainly two fold – test sites are used to apply in-situ calibration techniques on the one hand. On the other hand, another driving force is the empirical evaluation of sensor performance in true operational environments. Such performance tests are particularly necessary in case new sensors and systems become available. Since the advent of the new digital airborne imagers and their commercial availability, main attention in photogrammetric community was focused on the analysis of the systems' potential and their comparison to well-known analog mapping cameras. This is still the case: new commercial airborne systems are showing up and already available systems are modified through hardware and/or software. Empirical tests are done by the system vendors, in order to guarantee and validate the system's performance from test field results. In some cases, the sensors are independently analyzed by academic organizations. Other tests are done by potential customers before their final purchase decision is made. Furthermore, national mapping agencies, for example, are interested in a new sensor's performance to solve the question of whether the technology is able to fulfil present standards for map compilation.

Within this paper, main results and findings of one of those performance tests are given. In summer 2004 the ADS40 Aerial Digital Sensor from Leica Geosystems was flown in the Vaihingen/Enz test field close to Stuttgart, Germany, with more than 200 signalized and independently coordinated object points. These flights were part of a joint project of Leica Geosystems and the Institut für Photogrammetrie (ifp), Universität Stuttgart. The whole data processing and quality analysis was done at the ifp, i.e.: the evaluation of the geometric as well as the radiometric performance

and resolution. The results were obtained by using standard commercial Leica software as well as alternative processing approaches, and therefore reflect an independent estimation of the ADS40 performance from true flight data.
Within Sections 2 and 3 the Vaihingen/Enz test site and the mission flight design are given, followed by the presentation of empirical results in Section 4. Please note, only the results from geometric analysis based on the standard commercial process flow are given here. The results obtained from test flight data are discussed in Section 5.

2. The ifp test site Vaihingen/Enz

The ifp test site Vaihingen/Enz close to Stuttgart is an ideal test area for geometric accuracy analysis of airborne sensors. Within this area a sufficient number of signalized ground control points (GCP), coordinated from static GPS surveys, serve as independent check point (ChP) information to estimate the (absolute) quality of object point determination from airborne sensor data. The ground control point distribution for the 2004 mission flight campaign is given in Table 1. The accuracy of GCPs is in the 2cm range. The principal locations of signalized object points are based on the ideal point distribution for fully signalized medium-scale (1:13000) wide angle analog camera flights with 60% forward and side-lap conditions with some additional points in the western part of the test area. Besides these signalized points, manhole covers are additionally measured as natural targets. During the ADS40 flight mission mobile resolution targets (Siemens star, strip bar pattern) were fixed within the area, to empirically estimate the spatial image resolution from different heights.

#	Point type	# of points	Location of points
1	signalized/painted squares 1m x 1m	83	whole test site
2	signalized/painted squares 0.25m x 0.25m	62	western part of test site
3	well defined natural points (manhole covers)	69	whole test site

Table 1: Point distribution in test field Vaihingen/Enz.

The overall spatial extension of the test area is 7.5km (east-west) x 4.8km (north-south). The 3D visualization in Figure 1 gives an impression on land use and terrain undulation. The terrain heights range between 170m and 350m above mean sea level.

Figure 1: 3D view of ifp test site Vaihingen/Enz (height component 3x exaggerated).

Since 1995 the test field Vaihingen/Enz has been continuously used for a large number of well-controlled test flights. Besides the evaluation of system performance of integrated GPS/inertial components in combination with standard analog mapping cameras, a second goal was the quality estimation of new digital airborne sensors. Therefore, the potential of the very first digital airborne line scanners like DPA, WAAC and HRSC-A was investigated from this test site data, starting in the mid-1990s. Of the new commercial large format digital sensors, DMC and ADS40 were flown already. Besides this, medium format sensors, which may complement digital

large format airborne sensor systems in terms of higher flexibility for smaller acquisition areas at lower costs, have also been tested.

3. Test flight design

3.1 Test set-up

In summer 2004 the ADS40 was flown in the Vaihingen/Enz test field (one flight mission at June 26). The ADS40 sensor design was already described in several publications (i.e. Sandau et al. (2000)), only some very basic information is repeated here:

- focal length 62.5mm, field of view (across track) 46deg
- 10 linear CCDs in one focal plane, 12000 pixel each with 6.5μm x 6.5μm pixel size
- 3 pan-chromatic (PAN) channels (each using staggered CCD lines[1] (2 x 12000 pixel)) at nadir viewing and at 28deg (forward) and 14deg (backward) viewing angles
- 4 multi-spectral (MS) channels at 16deg forward (RGB) and 2deg (NIR) viewing angle

The flight mission itself was carried out by the Leica flight group. The ADS40 was installed in a Pilatus Porter aircraft which allows for very slow flying speeds. This is essential especially for ADS40 image data recording from very low flying heights. Altogether four different image blocks were acquired with different block geometries flown at different flying heights (Table 2). In all cases the long-strips were flown in east-west direction. The given ground sampling distance (GSD) is valid for non-staggered imagery. This GSD values are nominal values only, calculated from focal length and flying height above ground. The true spatial resolution of ADS40 has to be analyzed from resolution targets like Siemens star or special bar pattern. The analysis of spatial resolution of ADS40 and the influence of image staggering and image restoration on resolution improvement was another goal of this test campaign. This topic is not considered within this paper. An extended presentation and discussion of ADS40 spatial image resolution refinement was already given in Becker et al. (2005), Reulke et al. (2004).

#	flying height h_g [m]	image scale m_b	nominal GSD [m]	# long strips	# cross strips	Side lap % (east-west lines)	Side lap % (north-south lines)
1	4000	64000	0.42	1	2	-	48
2	2500	40000	0.26	3	3	70	29
3	1500	24000	0.18	4	2	44	-
4	500	8000	0.06	8	2	55	-

Table 2: ADS40 image block configurations (June 26, 2004).

[1] Within the later aerial triangulation (AT) processing image measurements from non-staggered images are considered only.

Figure 2: Aircraft installation ADS40 Vaihingen/Enz test flight (June 26, 2004).

It has to be mentioned, that different to the standard ADS40 system installation, two additional GPS/inertial units were installed during the flight. The influence on different GPS/inertial trajectory solutions on the final geometric object point quality was another topic of concern. Besides the standard ADS40 configuration including the Applanix POS (Mostafa et al. (2001)) using LN200 fiber-optic gyro based inertial measurement unit (IMU) (Litton)[2], the Applanix AIMU dry-tuned gyro system based IMU (part of the Applanix POS/AV-510 system and based on the Inertial Science Inc. DMARS IMU) and the IGI IMU-IId fiber-optic gyro unit, which is essential part of the IGI AEROcontrol-IId system (Kremer (2001)) was fixed to the ADS40. The IMU-IId is based on a Litef inertial unit. Since the rigid mount (no relative movements between camera and IMU) has to be guaranteed for all three systems during the whole flight mission, a special metal hat was constructed and fixed on top of the ADS40 electronics head as it can be seen in Figure 2. The two additional IMUs are mounted on top of this hat. The LN200 is on its standard position integrated inside the camera housing close to the CCD focal plane.

3.2 Theoretical accuracy of object point determination

The theoretical accuracy of object point determination is mainly dependent on the quality of image point measurements, the resulting base to height ratio and the individual block geometry. A first rough estimation on the aspired horizontal and vertical performance of object point determination can be obtained from the well known normal case conditions (1) (Kraus 2004):

$$\begin{aligned} \sigma_X &= \sigma_Y = m_b \cdot \sigma_B \\ \sigma_Z &= m_b \cdot \frac{h_g}{B} \cdot \sigma_B \end{aligned} \tag{1}$$

The horizontal accuracy σ_X, σ_Y is a function of image scale m_b and image point measurement accuracy σ_B. The vertical accuracy σ_Z is additionally influenced by the resulting base B to height h_g ratio. This base to height ratio is defined by the sensor's geometry. In case of ADS40 the base to height ratio is obtained from the 42deg angle between forward and backward looking channel. The accuracy of image point measurements affects horizontal as well as vertical components. Since all measurements in ADS40 imagery were done in the non-staggered images the image point accuracy is assumed to be within the 3μm level. This corresponds with the sigma naught from empirical bundle adjustment, without use of additional self-calibration parameters. With the use of additional parameters the sigma naught values are slightly better (about 2.5μm). From this, the theoretically object point accuracy $\sigma_X, \sigma_Y, \sigma_Z$ from normal case conditions for the different ADS40 flying heights can be obtained as follows (Table 3). In general, the theoretical object point

[2] Future ADS40 systems will be integrated with the GPS/inertial technology provided by Terramatics, Calgary. Their system, IPAS (Inertial Position and Attitude System), will substitute the formerly used Applanix POS GPS/inertial components (Flint 2005).

quality of horizontal and vertical components is close, due to the long image base of ADS40.

#	flying height h_g [m]	nominal GSD [m]	σ_X, σ_Y [m]	σ_Z [m]	m_{XY} [m]	m_Z [m]
1	4000	0.42	0.20	0.25	0.08	0.13
2	2500	0.26	0.12	0.15	0.04	0.06
3	1500	0.18	0.07	0.09	0.03	0.06
4	500	0.06	0.02	0.03	0.03	0.04

Table 3: Precision of object point determination.

Within the theoretical accuracy estimation based on normal case conditions, the influence of different image overlaps on block geometry is not taken into account. From that, these numbers might be too pessimistic for block configurations with strong overlap conditions. This individual image block geometry (so-called design factor) is represented in the structure of the normal equation matrix, from which the accuracy of estimated unknowns is obtained. Therefore, the estimated mean accuracy (precision) m_{XY}, m_Z for horizontal (XY) and vertical (Z) object coordinates is also added to Table 3. All numbers are scaled to a sigma naught value of 3μm. Comparing these numbers to the theoretical accuracy estimated from Equations (1), a certain discrepancy is obvious. Except from the 500m flight, the values from matrix inversion are about a factor of 2-3 less. This reflects the influence of strong image overlaps which are not considered in the formulas from stereo normal case with two-folded points maximum only. Besides the continuous 100% overlap in flight direction – which is inherent for all push-broom line scanners – the side-lap between neighboring strips is significant larger than the typically flown 20-30% (Table 2). This is due to the limited test site extension. In case of the 4000m and 2500m flying height blocks, additional cross strips which again do overlap each other are included, resulting in much stronger block geometry. All this positively influences the performance of theoretical object point determination. Please note that this in some cases quite large side-laps and the availability of additional cross lines might differ from later typical commercial flight configurations.

The theoretical accuracy estimation reflects the optimal accuracy obtained from error free data and given block geometry. The numbers have to be taken into account when the absolute empirical accuracy from check point analysis is discussed.

4. Experimental results

Within this section the results from ADS40 image triangulations and absolute accuracy checks in object space are presented. The results from all different flying heights are considered. The triangulations are based on the ORIMA/CAP-A software package which is one core module within the Leica ADS40 data process chain. The image coordinate measurements used in AT are obtained from automatic tie point transfer and manual measurements (for the signalized points).

In general, the orientation of push-broom line scanner imagery can be solved applying two different methodologies: The orientation fix point approach or

alternatively the method of direct georeferencing. Historically, the orientation fix point method was established to flexibly compensate for errors in the directly observed exterior orientation elements, provided by stand-alone inertial or integrated GPS/inertial units. This exterior orientation information was only used to interpolate the relative movement between the photogrammetrically obtained orientation fix points. The absolute sensor trajectory is still obtained from photogrammetric reconstruction using tie point measurements in three-line image geometry. This approach was originally proposed by Hofmann (1974). The orientation fix approach is implemented within the ORIMA/CAP-A software (Hinsken et al., 2002).

With the advent of small and compact integrated GPS/inertial systems of high performance, the direct measurement of exterior orientation with sufficient absolute accuracy became possible. Relying on such a high quality GPS/inertial trajectory solution, the remaining effort for AT decreases and is only necessary to determine a small number of additional unknowns for system calibration or remaining datum shift parameters. This can be done with a significantly reduced number of tie point measurements. From an operational point of view the knowledge of high-quality exterior orientation parameters simplifies and accelerates the photogrammetric reconstruction process. Mathematically, this approach is based on the philosophy of direct georeferencing of airborne sensors originated from research institutes like University of Calgary beginning of the 1990s (Schwarz et al., 1993).

Both variants of push-broom line scanner orientation and their influence in geometric object point accuracy have been applied and tested in the framework of this ADS40 performance test. Only the results from ORIMA/CAP-A triangulation will be covered in the following, due to space limitations. The direct georeferencing approach is implemented in the ifp bundle adjustment dgap. Some results from this processing are already given in Cramer (2005). In general, both orientation approaches offer quite similar performance, with some minor differences for the high altitude flights.

4.1 Additional tie point measurements in MS channels

The orientation of airborne imaging sensors typically is based on the manual and automatic measurement of image points. In case of push-broom scanners like ADS40, these image point measurements are mostly done in the pan-chromatic images only. Hence, the information from PAN channels is used to determine the sensor's trajectory. Based on the knowledge of these exterior orientations all other products are obtained, like ortho imagery or terrain models. Different to this traditional approach, automatic and manual tie and control points were measured in the color bands, additionally. This finally results in 10-folded overlapping points within one single image strip, namely PAN-A/B (forward, backward, nadir) and multi-spectral (red, green, blue, near infra-red). The number of image rays per point is even higher, if points are measured in overlapping regions of neighboring strips.

For the 1500m flight block this influence of additional tie point observations from MS channels on object point accuracy was analyzed and compared to the approach based on image point measurements in three PAN-A channels only. Since all other adjustment parameters remain unchanged, the variations in object space are directly linked to the different image point measurements. Without going into detailed

analysis here, almost no increase in object point accuracy becomes visible when using additional observations from MS channels. In some cases the performance of point determination in one coordinate component even decreases slightly, in other cases an accuracy increase in one coordinate component of 20% can be seen. This is entirely dependent on the number of used GCPs.

The exclusive use of pan-chromatic channels seems to be sufficient for ADS40 orientation, the geometry of image ray intersection is mainly defined by the angle between forward and backward looking pan-chromatic channels. No general increase in object point accuracy is visible when using observations from additional channels.

4.2 Quality of real-time trajectory solution

Within the following the influence of real-time GPS/inertial trajectory solution on object point performance is compared to the standard post-processed trajectory solution. Real-time trajectory processing in general could be relevant for highly time stringent data processing. Theoretically, such trajectory information could even be generated (close to online demands) during the flight mission itself. As soon as such trajectory information is available, the rectification of ADS40 imagery can also be done with very short time delays from mission ending or aircraft landing.

Please note that the real-time solution described here is not “truly” real-time: The processing was done after the flight. Within trajectory computation the forward Kalman filtering was also amended by a backward smoothing process, which can only be applied when all GPS/inertial data are present, i.e.: the mission flight was finished completely. The trajectory is based on GPS C/A code observations only, without using (real-time/post-processed) differential corrections provided from standard reference stations or real-time correction services. Within the following, this solution will be denoted as *quasi* real-time.

If such *quasi* real-time trajectory solution is used for ADS40 image rectification and automatic tie point transfer, the number of matched points is about 25% less compared to the tie point transfer using the post-processed GPS/inertial trajectory result. This is due to the more correct exterior orientation parameters after post-processing, which is mainly influenced from the use of differential GPS phase observations. In case of the ADS40 1500m image block the number of matched image points increases from 1600 to 2000 when using the post-processed GPS/inertial trajectory. Using the *quasi* real-time solution within ORIMA/CAP-A bundle adjustment afterwards, the accuracy (RMS) in object space is about 10-15cm for horizontal and 30cm for vertical object point components. This performance is obtained from 192 check points and based on the use of 12 GCP. GPS/inertial data is provided from standard LN200 system input.

Nevertheless, comparing this absolute accuracy from check point analysis to the theoretically numbers from Table 3, these values are significantly worse for horizontal and vertical coordinate components, respectively. This indicates that even though the orientation fixes approach in general offers a very flexible tool to handle direct exterior orientation parameters with different performance, the accuracy of

quasi real-time GPS/inertial trajectory computations is not sufficient for highest accuracy demands. As shown above, decimeter accuracy should be possible with use of a certain number of ground control points. With additional real-time differential GPS correction services this accuracy level should also be possible even with a reduced number of GCP. From this, there might be a number of applications, where such a processing approach seems to be worthwhile to follow.

4.3 Performance based on post-processed trajectory solution

The ORIMA/CAP-A triangulation using the LN200-derived GPS/inertial trajectory solution matches the standard flow of ADS40 data processing. Until recently LN200 IMUs have been part of the standard ADS40 sensor system equipment and installation. Within the following the performance of object point determination is given, based on the LN200 post-processed trajectory information. Results from 3 different flying heights (excluding the very low altitude flight, which is presented in Section 4.5) are given. Three different processing configurations are considered: ORIMA/CAP-A triangulation based on 12, 4 and 0 GCPs, respectively. Within the first tests, no additional self-calibration is included in AT process. In addition to the inherent object coordinate unknowns, additional boresight misalignment parameters (reflecting the physical misalignment between IMU body frame and camera photo coordinate frame) and block-wise position offset and drift parameters are estimated as additional unknown parameters during adjustment only. Note, that position offset and drift parameters can only be considered as far as (at least one) GCP is introduced.

The RMS values for all three checked control point configurations and three flying heights are depicted in Figure 3. These values are obtained from independent check point analysis. Dependent on the flying height (not all check points are visible in all flying heights) up to 202 check points have been available, also influenced from the number of GCP. Table 4 gives the exact numerical values for the 12 GCP configurations, each. The empirical values reflect the absolute accuracy of object point accuracy and have to be related to the nominal GSD, as well as the theoretically expected accuracy discussed earlier and previously depicted in Table 3.

Figure 3: Accuracy of object points (RMS) based on LN200.

#	flying height h_g [m]	#ChP	RMS (**no** self-calibr.)			RMS (**with** self-calibr.)		
			ΔEast [m]	ΔNorth [m]	ΔVert. [m]	ΔEast [m]	ΔNorth [m]	ΔVert. [m]
1	4000	134	0.067	0.075	0.123	0.063	0.057	0.107
2	2500	182	0.066	0.065	0.100	0.064	0.059	0.087
3	1500	190	0.052	0.054	0.077	0.031	0.040	0.057

Table 4: Accuracy from check point analysis (12 GCP, ORIMA/CAP-A, LN200).

In general, the absolute accuracy from check point analysis shows a certain (but relatively small) degradation with increasing flying height, as it should be expected. As far as GCPs are included into adjustment, the horizontal accuracy is very consistent and well within the 5-8cm level (for each component) even for higher

flying heights. The vertical component ranges between 8cm and 12cm. This coincides to an accuracy of about 1/3 to 1/5 of a pixel in object space, dependent on the flying height. With only one exception (vertical component of 1500m flight) the use of 12 or 4 GCPs is of almost no influence on the object point accuracy, illustrating that 4 GCPs are sufficient to control the analyzed block configurations.

If the empirical accuracy is compared to the estimated values from normal case conditions (Table 3), all expectations are more than fulfilled. Comparing the RMS values to the more stringent precision including the individual block geometry, the performance of ADS40 differs from expectations - mainly for the 1500m and 2500m flight, as long as no self-calibration is taken into account. Considering the 12 GCP case only, the empirical accuracy of 7cm (horizontal) from the 1500m block is compared to the estimated precision of 3cm (horizontal). For the 2500m block the horizontal RMS is 9cm, this value has to be compared to the 4cm precision from theory. For the 4000m block the empirical horizontal accuracy of 0.10m corresponds to the theoretical precision of 0.08m. Within the vertical component the RMS of 12cm almost exactly matches the theoretical precision for 4000m flight. For 2500m and 1500m again the vertical accuracy is slightly worse: the empirically obtained 8cm and 10cm accuracy for 1500m and 2500m flights respectively is compared to the 6cm precision.

This situation changes using additional parameters for self-calibration within the ORIMA/CAP-A adjustment process. As it can be seen from the RMS values in the second half of Table 4, an increase in absolute accuracy is obvious. In all coordinate components the RMS values are less, the accuracy increase reaches up to 2cm. Now the empirical accuracy is closer to the estimated precisions from Table 3. For vertical components these demands could be fulfilled. The horizontal accuracy still remains slightly worse, indicating that there still might be some small and non corrected systematic effects within the sensor data.

The AT cases using no ground control points have to be considered separately. For sure, those evaluations are non standard and, even more important, without any external check information no control of absolute accuracy of the whole AT process is possible. From geodetic point of view such no redundancy configurations have to be avoided strictly. Nevertheless, in some cases such processing approaches might be desirable or even inevitable. Keeping the non redundancy problem in mind, the already depicted results for 0 GCP configurations (Figure 3) are discussed like follows. The accuracy (RMS) is significantly worse compared to the AT versions using GCP, nonetheless, the horizontal accuracy still remains within a quite acceptable 15cm level. This accuracy is more or less independent from actual flying height, which might indicate that the accuracy is mostly deteriorated from systematic (position) offsets, which cannot be corrected as long as no exterior control information is available. The performance of vertical component is different. Dependent on the flying height the accuracy performance decreases to 15cm, 30cm, 40cm accuracy level for 1500m, 2500m, 4000m flying height, respectively. This accuracy behavior might be due to the two following effects, where a clear separation between the two is almost impossible:

1. The absolute accuracy of object point determination is essentially dependent on the absolute accuracy of the dGPS/inertial trajectory, which itself is based on the absolute performance of prior dGPS-processing. Without using any GCP, remaining trajectory offsets will directly be transformed to global shifts in object point coordinates.
2. Any non corrected systematic errors from image space might influence the performance of object points. Especially the height component is susceptible to such errors. Since such influences are scale dependent their amount will increase with higher flying heights.

Within Figure 4 the residuals from check points are plotted for the 2500m flight, where the results from the configuration based on no ground control points (left) are compared to the results using 4 GCP located in the corner of the block (right), exemplarily.

Figure 4: Residual vectors in object space (2500m, LN200)
(0 GCP case (left), 4 GCP case (right))

The clearly systematic horizontal and vertical component differences are quite obvious. All residual vectors of horizontal components are almost pointing towards the south-east direction, whereas all vertical differences are positive. The mean offsets are about 10cm, -8cm and 31cm for east, north and vertical residual components. The variation of differences from this mean values (STD) is within 0.077m (east), 0.070m (north), 0.096m (vertical) only, which is similar to the accuracy (RMS) when using 4 GCPs in the corners of the block, as depicted in the second half of the figure. This indicates that with the use of a very limited number of ground control points only, the major part of these systematic errors can be corrected, which will increase the accuracy significantly. In the ideal case – if the difference at one available check point exactly matches the mean offsets – the STD values mentioned above should be obtained as RMS accuracy.

4.4 Performance based on non-standard IMU trajectory solutions

All results presented thus far are based on the standard system components which are part of the commercially available ADS40 installation. In addition to that, the influence of different IMU data on the overall object point performance could be investigated when using different IMUs for the GPS/inertial data integration; this is one essential processing step for the evaluation of line imagery in general. In this specific test flight additional IMU data were obtained from the Applanix AIMU and the IGI IMU-IId, which are used as essential parts of the Applanix POS/AV-510 and the IGI AEROcontrol-IId integrated GPS/inertial system, respectively. Using the AIMU based data for the ORIMA/CAP-A triangulation of images the following results (RMS) could be obtained (see Figure 5). Within Figure 6 the corresponding results (RMS) are plotted for the AEROcontrol IMU-IId based integrated system. These figures should be compared to Figure 3, which depicts the performance (RMS) of the standard ADS40 LN200 installation discussed before. In all cases, no self-calibration

is applied. Besides the standard unknown parameters only misalignment angles and position offset/drift parameters are introduced.

Figure 5: Accuracy (RMS) of object points based on AIMU.

Figure 6: Accuracy (RMS) of object points based on IMU-IId.

#	flying height h_g [m]	#ChP	RMS **AIMU** based solution			RMS **IMU-IId** based solution		
			ΔEast [m]	ΔNorth [m]	ΔVert. [m]	ΔEast [m]	ΔNorth [m]	ΔVert. [m]
1	4000	134	0.072	0.068	0.116	0.075	0.063	0.137
2	2500	182	0.073	0.066	0.096	0.069	0.071	0.088
3	1500	190	0.054	0.050	0.067	0.056	0.042	0.061

Table 5: Accuracy from check point analysis (12 GCP, ORIMA/CAP-A, no self-calibration).

Both trajectory solutions in general show a quite similar accuracy behavior, which is almost independent on the IMU used. Especially when comparing the two results given in Table 5, obtained from analysis of the exemplarily chosen 12 GCP based adjustments, the consistency between both solutions is obvious. There is no significant difference visible for both solutions, which is even more evident, when the obtained standard deviations are considered (not depicted here). These values somehow represent the noise level which for both systems is very consistent and similar. Furthermore, comparing the numbers from Table 5 to the values given in Table 4 (no self-calibration case only), no big difference in the three evaluated solutions becomes obvious, although the absolute performance of the LN200 should be less compared to the two other IMUs. This clearly indicates the high versatility of the orientation fix point approach, to a certain amount to handle GPS/inertial data of different performance. This was exactly the reason for developing such an approach originally.

The obtained performance from the no ground control point based solutions again has to be discussed in some more detail. From Figure 5 and Figure 6 differences in object point accuracy are clearly obvious. The IMU-IId based solution obtains better results for the 2500m and 1500m flight configurations compared to the AIMU trajectory. Such an effect is most likely due to different absolute accuracy of GPS/inertial trajectory results, which itself is based on the absolute performance of prior dGPS processing (already mentioned in Section 4.3). Within the context of the ADS40 test campaign two independent dGPS solutions were calculated and involved in GPS/inertial trajectory computations. The two dGPS and integrated trajectory solutions mainly differ by absolute offsets of approx. 5cm and 2cm for vertical and north component, respectively. This is due to a slightly different choice of dGPS processing parameters from two individual users. The first dGPS processing result was used for the LN200 and AIMU data integration. The second, independently calculated dGPS trajectory was feed in the IMU-IId based integrated trajectory

computation. Since the quality of dGPS trajectory is essential for the quality of the integrated solutions (mainly for the positioning component) any errors in the dGPS solution are directly shifted in the integrated solution. Such offsets cannot be compensated without any GCP and so they become obvious in check point differences, especially in vertical component. The difference between AIMU and IMU-IId vertical accuracy is clearly visible and exactly matches the difference between the two different dGPS trajectory results. This nicely illustrates possible problems when using no external control information.

Quite interesting to note: for the high altitude 4000m block, the individual performance of IMU-IId and AIMU based solutions is again very similar, as it already was the case for the GCP based adjustments. Although the absolute shift in dGPS and GPS/inertial trajectories is also present here, this effect is overlaid from other systematic effects most likely due to remaining scale dependent errors from image space, as already mentioned.

4.5 Performance from very low altitude flights

The performance of ADS40 from very low altitude flights is considered within this part of the paper. A 500m flying height block was initiated in order to empirically analyze the system performance at the limit of smallest realizable pixel size in object space. Due to the very low flying height only PAN imagery was available, the short image data integration time was not sufficient for recording of color imagery. Hence, only automatic tie and manual points from PAN channels were used during processing. Besides that, the processing was done similarly to the already presented image blocks from 1500m-4000m altitude. Again the ORIMA/CAP-A results are presented only, no additional self-calibration is included, only boresight misalignment and block-wise position offset and drift is used as additional unknowns in AT.

Unfortunately, due to erroneous mission flight planning, the 500m block was partly flown outside the original Vaihingen/Enz test site boundaries. In order to provide sufficient number of check and control points for independent evaluation of the ADS40 500m flight, even though 2/3 of the block were without the original test site area, additional object points have been re-measured after flight to extend the test area. This re-definition of natural points is a quite difficult task due to the lack of clearly identifiable natural points in the mostly rural country side covered by the test site. Such larger uncertainty of image point definition will be of negative influence on the later object point accuracy and has to be considered within analysis of this flight mission.

#	#GCP	#ChP	RMS		
			∆East [m]	∆North [m]	∆Vert. [m]
1	12	68	0.064	0.047	0.035
2	4	76	0.064	0.047	0.034
3	0	80	0.065	0.070	0.042

Table 6: Accuracy from check point analysis (500m flight, ORIMA/CAP-A, no self-calibration).

The estimated absolute accuracy (RMS) from check point differences is given in Table 6. It is quite interesting to see, that in case of the 500m block the height performs better than the horizontal component. This is due to the additional error in point identification caused by the need for re-measurement of natural targets. If one assumes only small object height variations, valid for a certain area around the natural point used as check point, the sub-optimal measurement in image space will mostly influence the horizontal accuracy component of object points.

From Table 3, a theoretical accuracy in the range of 3cm and 4cm should be expected for this block configuration. For horizontal components this accuracy potential could not be reached, which again shows the effect of point identification error. Different to the horizontal coordinates, the height accuracy fulfills these stringent demands.

Quite remarkable to see, the no ground control point case is of almost similar quality than the versions using GCPs. Only a very small decrease in accuracy is present for vertical and north component. This somehow is in conflict to the findings before, where the effect of absolute position shifts in dGPS and GPS/inertial trajectory was discussed. In theory these effects should be large enough to become visible in the 500m block also.

With the use of additional self-calibration parameters, again a small increase in horizontal components is possible. For the 12 GCP based solution for example the accuracy after self-calibration is within 5.5cm, 4.5cm and 4.2cm for east, north and vertical component, respectively.

5. Discussion of results

The investigations have shown the high geometrical system performance of ADS40. The accuracy is obtained from independent check point differences. For the standard LN200 based system installation using a sufficient number of GCPs during adjustment with additional self-calibration, the obtained accuracy is in the range of 1-2µm·m_b for horizontal and 0.03-0.05‰ of flying height for vertical components. These numbers are obtained from the 1500m-4000m flights, and they are related to absolute accuracy in object space. The 500m flight performs different; the obtained accuracy is within 9µm·m_b horizontal and 0.07‰ of flying height for vertical component only. A certain amount of this deterioration has to be allocated to the non-optimal choice of control and check point information, as already explained. Further tests are necessary to verify the low altitude performance of ADS40.
Except of this, ADS40 fulfills and in some cases even more than fulfills the typical geometrical accuracy requirements of airborne imaging and can well be used for photogrammetric surveys.

The standard ADS40 process flow using the ORIMA/CAP-A bundle approach is reliable and fulfills all requirements. Alternative bundle adjustment based on direct georeferencing is also possible. Both approaches are of almost similar performance,

at least as long as a reliable GPS/inertial trajectory solution of sufficient accuracy is available.

It is shown that the geometrical performance of object point determination is mainly defined by the stereo angle of forward and backward looking ADS40 pan-chromatic image channels. The additional measurement of image points in MS channels does not significantly increase the accuracy in object space. From that the exclusive use of pan-chromatic image channels seems to be sufficient for ADS40 orientation.

The three tested GPS/inertial trajectory solutions based on different IMU data are of almost similar performance at least as long as additional GCPs are introduced into aerial triangulation. The remaining differences in the obtained object point quality are only marginal. Nevertheless, for control point free evaluations, there is no way to correct for remaining global errors in GPS/inertial trajectories. From that special attention has to be drawn on the processing of GPS/inertial and dGPS trajectories. Since the direct georeferencing approach relies on accurate and consistent GPS/inertial results, the careful processing of GPS data is especially relevant for this method. Nevertheless, even for the ORIMA/CAP-A orientation fix approach a certain quality of GPS/inertial trajectory has to be guaranteed (see results from *quasi* real-time GPS/inertial trajectory solution).

Experiences during processing of this test flight data have shown, that even though the processing of dGPS trajectories was done with sufficient care, two independent dGPS trajectory results were obtained from two individual software users. Both results differ by an almost constant offset in the range of a few centimeters. These differences are not dependent on the different manufacturers' system components, but most likely due to slightly different choice of parameter settings during dGPS processing. Although such effects are small (close to GPS noise level) they have to be taken into account for highest accuracy demands, especially when using 0 GCPs. As soon as GCPs are involved, those systematic offsets are compensated in AT. Nevertheless, with less optimal GPS constellations or less careful dGPS processing, which might happen in a production environment with stringent time constraints, such dGPS trajectory offsets (in some cases even larger and overlaid with drift effects) should be expected. Hence, the use of a certain number of control points is highly recommended, to compensate for such effects in operational data processing.

The topic of self-calibration and overall system calibration is of special concern when GPS/inertial components are used as one essential part of any airborne sensor system. Within standard ground control point based AT, the exterior orientations are estimated optimally but do not necessarily represent the physically valid camera stations and orientation angles. In difference to that, GPS/inertial sensors now provide direct measurements of physical exterior orientation parameters. To avoid conflicts, the calibration of the whole sensor system should be obtained from in-situ calibration approaches. From the flights investigated here, the use of misalignment angles and position offset (and drift) parameters was necessary. Besides that only a small increase in object point accuracy was obtained by adding additional self-calibration parameters. This indicates that the already applied calibration parameters

from a priori calibration are close to optimal for this mission flight, which gives hints on the high internal system stability.

Within the analysis, the automatic tie point transfer was done based on two different GPS/inertial trajectory solutions. Most of the tie point matching was based on the *quasi* real-time GPS/inertial trajectory. Even though such integrated trajectory information is not sufficient for high performance photogrammetric point determination, the results from tie point matching are acceptable. If the matching is repeated with a post-processed GPS/inertial trajectory the number of matched tie points is increased, but this is of almost no influence on object point accuracy from ORIMA/CAP-A.

Quasi real-time GPS/inertial processing using single point GPS trajectory solution allows for object point accuracy, which is a factor of 2-3 worse compared to the solution based on post-processed GPS/inertial trajectory. This is not acceptable for highest accuracy demands; nevertheless such performance might be sufficient for certain applications, especially if the focus is on very time stringent data evaluations. Furthermore, using already available real-time differential correction services will positively influence the performance of GPS/inertial trajectories. From that the accuracy of object point determination should also be increased. Such topics might become relevant for very time demanding applications like disaster monitoring.

6. Conclusion

Within this study the geometrical performance of ADS40 was analyzed in detail. All results are based on the empirical test flight material acquired from the Vaihingen/Enz test flight at June 26, 2004. The potential of standard ADS40 system installation and process flow was analyzed and verified from different flying heights. The results are obtained from independent check point analysis. These results are statistically relevant. The transfer to other mission flights with similar flight conditions should be possible. The general concept of push-broom airborne scanners again was proven from this empirical test analysis.

Acknowledgments

The author gratefully would like to thank all persons involved in this study. Special thanks needs to be expressed to Leica Geosystems for financial support of this test campaign.

Bibliography

Becker, S., Haala, N. & Reulke, R. (2005): Determination and improvement of spatial resolution for digital aerial images, Proceedings ISPRS Workshop on High Resolution Earth Imaging, Hannover, May 17-20, 2005, digitally available on CD, 6 pages.

Cramer, M. (2005): 10 Years ifp test site Vaihingen/Enz: An independent performance study, in D. Fritsch (ed.): Photogrammetric Week ’05, Wichmann, Karlsruhe, pp. 79-92.

Flint, D. (2005): Innovations to increase productivity of airborne sensors, in D. Fritsch (ed.): Photogrammetric Week ’05, Wichmann, Karlsruhe, pp. 69-77.

Hofmann, O. (1974): Studie über voll-elektronische Satellitenbild-Aufnahmesysteme im sichtbaren und nahen Infrarotbereich, Band I und II, durchgeführt von Messerschmidt- Bölkow-Blohm.

Hinsken, L., Miller, S., Tempelmann, U., Uebbing, R. & Walker, S. (2002): Triangulation of LH Systems' ADS40 imagery using ORIMA GPS/IMU, IAPRS, Vol. XXXIV, Part 3A, Graz, Austria, 7 pages, digitally available on CD-Rom.

Kraus, K. (2004): Photogrammetrie, Band I, Walter de Gryter, Berlin, 516 pages.

Kremer, J. (2001): CCNS and AEROcontrol: Products for efficient photogrammetric data collection, in Fritsch/Spiller (eds.): Photogrammetric Week '01, Wichmann, Karlsruhe, pp. 85-92.

Mostafa, M., Hutton, J. & Reid, B. (2001): GPS/IMU products – the Applanix approach, in Fritsch/Spiller (eds.): Photogrammetric Week '01, Wichmann, Karlsruhe, pp. 63-83.

Reulke, R., Tempelmann, U., Stallmann, D., Cramer, M. & Haala, N. (2004): Improvement of spatial resolution with staggered arrays as used in the airborne optical sensor ADS40, in Proceedings ISPRS congress, Istanbul, July 2004, digitally available on CD, 6 pages.

Sandau, R., Braunecker, B., Driescher, H., Eckhardt, A., Hilbert, S., Hutton, J., Krichhofer, W., Lithopoulos, E., Reulke, R., Wicki, S. (2000): Design principles of the LH Systems ADS40 airborne digital sensor, IAPRS, Vol. XXXIII, Part B1, Amsterdam, Netherlands, 8 pages, digitally available on CD-Rom.

Schwarz, K. P., Chapman, M., Cannon, M. & Gong, P. (1993): An integrated INS/GPS approach to the georeferencing of remotely sensed data, Photogrammetric Engineering and Remote Sensing PE&RS, Vol. 59, No. 11, pp. 1667-1674.

Captions of Figures

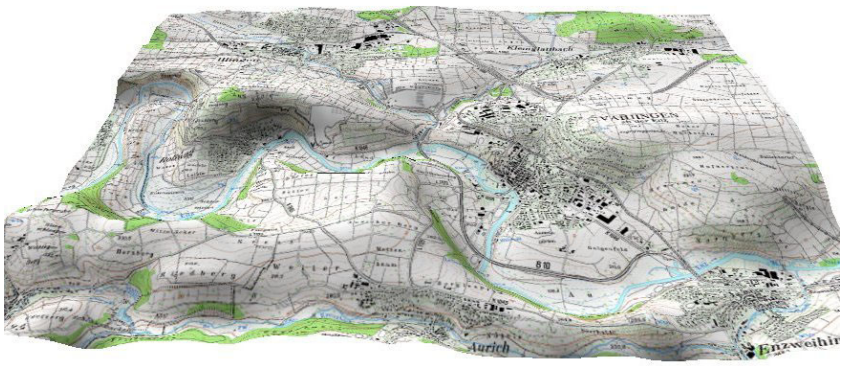

Figure 1: 3D view of ifp test site Vaihingen/Enz (height component 3x exaggerated).

Figure 2: Aircraft installation ADS40 Vaihingen/Enz test flight (June 26, 2004).

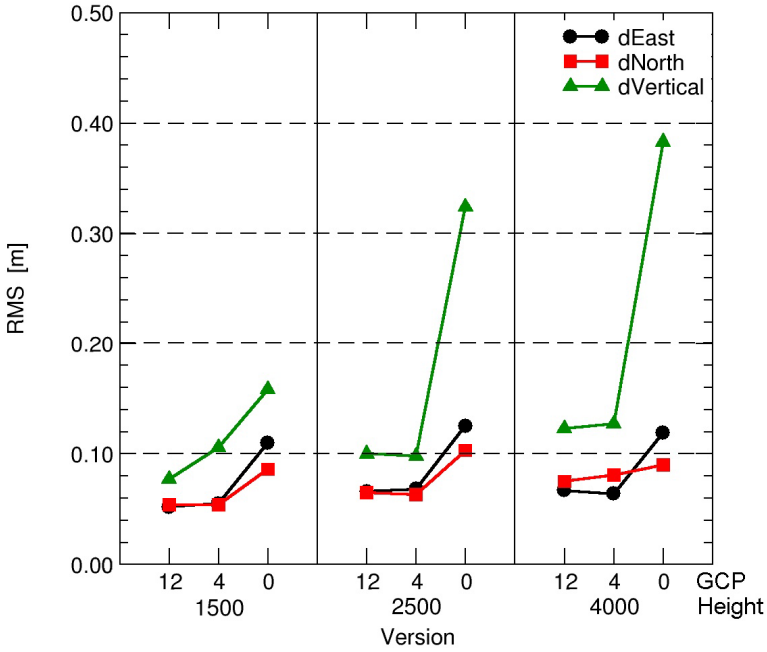

Figure 3: Accuracy of object points (RMS) based on LN200.

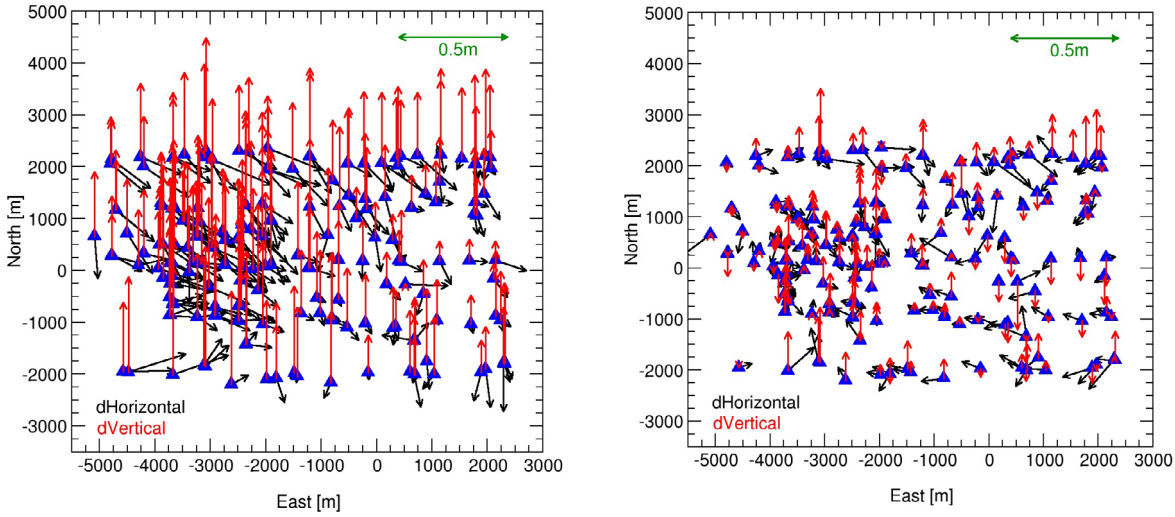

Figure 4: Residual vectors in object space (2500m, LN200)
(0 GCP case (left), 4 GCP case (right))

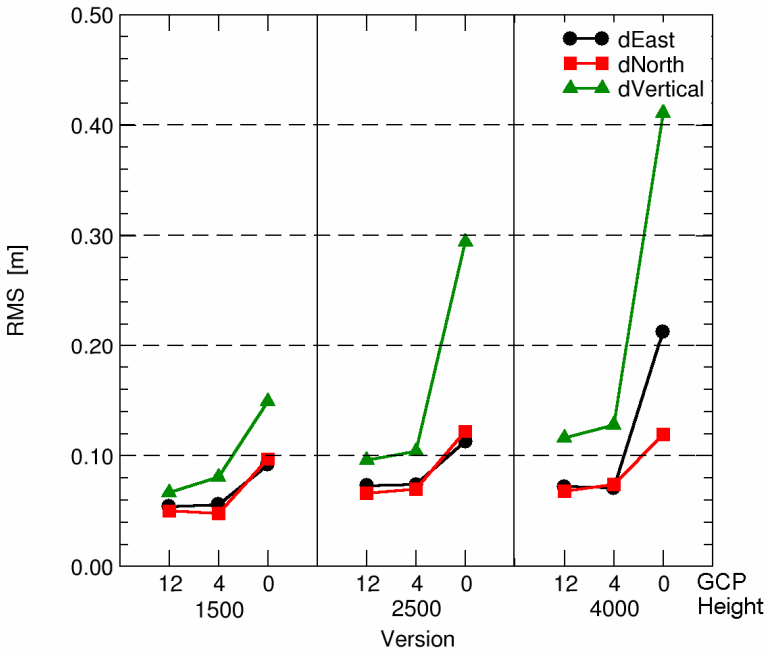

Figure 5: Accuracy (RMS) of object points based on AIMU.

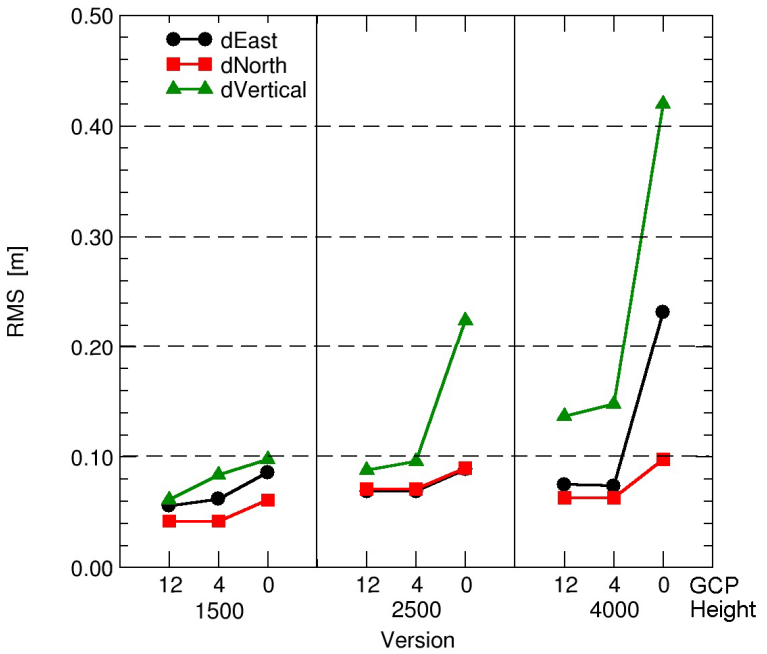

Figure 6: Accuracy (RMS) of object points based on IMU-IId.